Journal of Pure and Applied Sciences (JPAS),
Volume 2, Issue 2, Page 111-123, 2026

Cadmium-Free Buffer Layer Engineering for Spray-Deposited Cu_2ZnSnS_4 Thin-Film Solar Cells Using ZnS

F. O. Oluyemi[1*], G. M. Adesunloro[2], O. D. Itakorode[3]

[1,2,3]Department of Physics with Electronics, The Federal Polytechnic Ado-Ekiti, Ekiti State, Nigeria.
*Corresponding author (Email: oluyemifolasade886@gmail.com)

ABSTRACT

The development of a cadmium-free buffer layer for Cu_2ZnSnS_4 (CZTS) thin-film solar cells, using spray-pyrolyzed ZnS in place of toxic CdS was reported in this study. CZTS absorber films (bandgap ~1.45 eV) were deposited by spray pyrolysis from Cu:Zn:Sn = 1:1:1 precursor, and Cd-free ZnS (bandgap ~3.6 eV) buffers were co-spray-deposited on ZnO-coated ITO substrates. The fabrication and characterisation of an ITO/ZnO/ZnS/CZTS/Ag device are described. Structural and optical analyses confirm pure kesterite CZTS (no significant Cu_2SnS_3 or ZnS secondary phases) and a transparent ZnS layer. The ZnS buffer film exhibited high visible transmittance (>90%) and a direct bandgap of ~3.6 eV. The completed solar cell achieved Voc= 0.62 V, Jsc= 18.5 mA/cm², fill factor ~0.63 and efficiency η = 7.2%. These results (which surpass many previous CZTS/ZnS devices) demonstrate that spray-deposited ZnS is a viable Cd-free buffer, with performance improvements attributed to its wide bandgap and high transparency. Key findings include the confirmation of ZnS structural properties (XRD, Raman, SEM) and the reconciliation of previously inconsistent performance values.

***Keywords*— Cadmium-free buffer layer, CZTS, interface engineering, photovoltaic efficiency, spray pyrolysis, thin-film solar cells, ZnS**

I. INTRODUCTION

The increasing global demand for sustainable energy technologies has intensified research into thin-film photovoltaic materials that combine high performance with low environmental impact. Among emerging absorber materials, kesterite Cu_2ZnSnS_4 (CZTS) has attracted considerable attention because it is composed entirely of earth-abundant, low-cost, and environmentally benign elements. CZTS exhibits a direct optical bandgap in the range of 1.4–1.6 eV and a high absorption coefficient exceeding 10^4 cm^{-1}, making it highly suitable for solar energy conversion in thin-film devices [1], [2], [3]. Furthermore, unlike Cu(In,Ga)Se_2 (CIGS) and CdTe technologies, CZTS does not rely on scarce indium, gallium, or toxic cadmium, thereby offering significant advantages in terms of long-term sustainability and large-scale deployment.

Despite these advantages, the efficiency of CZTS solar cells remains substantially below the theoretical Shockley–Queisser limit. The current performance limitations are primarily attributed to high defect densities, secondary phase formation, non-radiative recombination losses, and interface-related defects at the absorber/buffer junction [4], [5], [6]. Consequently, considerable research efforts have focused on interface engineering and optimization of the buffer layer to improve carrier separation and reduce recombination losses.

Traditionally, cadmium sulfide (CdS) has been employed as the n-type buffer layer in CZTS solar cells due to its favorable heterojunction properties and well-established deposition techniques. However, CdS possesses several drawbacks, including toxicity, environmental concerns during fabrication and disposal, and a relatively narrow optical bandgap of approximately 2.4 eV, which results in parasitic absorption of short-wavelength photons [7], [8]. These limitations have motivated extensive research into cadmium-free alternatives capable of maintaining favorable band alignment while improving optical transparency.

Over the last decade, several cadmium-free buffer materials have been investigated for kesterite photovoltaics, including Zn(O,S), In_2S_3, ZnMgO, TiO_2, $Zn_{1-x}Sn_xO_\gamma$, and pure ZnS [9], [10], [6], [11], [12]. Zn(O,S) has demonstrated improved conduction band alignment but often suffers from compositional instability and process complexity. In_2S_3 provides good transparency but may require high-temperature processing and precise stoichiometric control. ZnMgO has emerged as a promising window/buffer material owing to its tunable bandgap; however, its deposition typically requires sophisticated sputtering equipment and careful control of Mg incorporation. TiO_2-based buffers have also been explored but frequently exhibit unfavorable interface states and increased series resistance. Consequently, identifying a low-cost, scalable, and environmentally benign alternative remains an active area of research.

Among the candidate materials, zinc sulfide (ZnS) has emerged as one of the most attractive Cd-free buffer layers for CZTS solar cells. ZnS possesses a wide direct bandgap of approximately 3.6–3.8 eV, excellent optical transparency in the visible region, and chemical compatibility with sulfide absorbers [13], [3]. Several studies have demonstrated that ZnS can successfully replace CdS while reducing optical losses associated with buffer-layer absorption [14], [12], [15]. Nevertheless, device efficiencies obtained using ZnS buffers remain highly dependent on deposition technique, interface quality, and conduction band alignment at the CZTS/ZnS heterojunction.

Band alignment between the absorber and buffer layer is particularly critical for achieving efficient carrier extraction. Numerical and experimental studies have shown that CZTS/CdS interfaces generally exhibit a

small conduction band offset that facilitates electron transport but may still contribute to interface recombination. In contrast, CZTS/ZnS interfaces can exhibit either a favorable spike-like alignment or an excessive conduction band barrier depending on deposition conditions and stoichiometry [16], [17], [11], [18]. Therefore, understanding and controlling the interface properties of CZTS/ZnS heterojunctions remains essential for improving device performance.

The deposition technique also plays a major role in determining the structural and optoelectronic properties of CZTS absorbers and ZnS buffer layers. Spray pyrolysis is particularly attractive because it is inexpensive, scalable, compatible with large-area manufacturing, and capable of depositing multiple device layers using a single equipment platform. Several authors have reported successful spray-deposited CZTS thin films exhibiting suitable crystallinity, bandgaps, and photovoltaic activity [19], [20], [21], [22], [23]. However, comparatively few studies have explored fully spray-deposited CZTS/ZnS heterojunction solar cells in which both the absorber and buffer layers are fabricated using spray pyrolysis.

Accordingly, this work investigates ZnS as a cadmium-free buffer layer for spray-deposited CZTS thin-film solar cells. Unlike previous studies that focused primarily on absorber characterization, the present work provides detailed structural, optical, and morphological characterization of both the CZTS absorber and ZnS buffer layers. Particular attention is given to ZnS phase formation, optical transparency, and surface morphology, as these properties directly influence heterojunction quality and photovoltaic performance. By employing spray pyrolysis for deposition of both layers, this study demonstrates a low-cost and scalable fabrication route toward environmentally benign CZTS-based photovoltaic devices.

II. MATERIALS AND METHODS

A. CZTS Precursor Solution

Analytical-grade copper(II) acetate monohydrate, zinc(II) acetate dihydrate, and tin(II) chloride dihydrate were each dissolved in deionised water at 0.025 M concentration. These metal solutions were then mixed in equal volumes, yielding a Cu:Zn:Sn molar ratio of 1:1:1. (This Cu-poor composition is intentionally lower than the stoichiometric 2:1:1 ratio of Cu_2ZnSnS_4, to suppress formation of Cu-rich secondary phases.) Separately, thiourea (CH_4N_2S) was dissolved at 0.20 M to supply sulfur, resulting in an S:(Cu+Zn+Sn) atomic ratio of about 2.67:1 (sulfur in excess). The mixed solution (pH ≈ 3) was stirred at ambient temperature for 1 hour before use.

B. CZTS Thin-Film Deposition and Annealing

Spray pyrolysis was performed using ultrasonic atomisation. Ultrasonically cleaned soda-lime glass slides were held at ~350 °C on a heated stage, a typical temperature for CZTS formation by spray. The mixed CZTS precursor solution was sprayed at ~5 mL/min with a carrier air flow of 2 L/min and a nozzle-to-substrate distance of ~15 cm. The spray was applied in multiple passes (~10 cycles), with the substrate reheated between passes to maintain 350 °C. The resulting film thickness was ~500 nm (measured by stylus profilometry). Immediately after deposition, the films were annealed in a tube furnace at 350 °C for 30 minutes under flowing N_2 gas. (Annealing in nitrogen avoids oxidation and decomposition issues that occur for CZTS when heated in air above ~300 °C.).

C. ZnS Buffer Layer Deposition

A thin intrinsic ZnO layer (~50 nm) was first deposited on the ITO to serve as a window layer and to improve junction formation. This was done by spraying a 0.5 M zinc acetate solution (in deionized water) onto ITO at 150 °C, followed by brief annealing. Then, the ZnS buffer was deposited by spray pyrolysis onto the ZnO-coated substrates. The ZnS precursor was prepared by dissolving zinc(II) acetate (0.075 M) and thiourea (0.225 M) in a mixed solvent of ethanol and water (ratio 1:4 by volume). (Ethanol was used to aid wetting and control droplet evaporation.) The substrate was maintained at ~350 °C, and the solution was sprayed at the same rate (5 mL/min, 2 L/min carrier air) and distance (15 cm) as for CZTS. After deposition of ~100 nm of ZnS (estimated by powdering a test film), the ZnS layer was annealed at 350 °C for 20 minutes in N_2.

D. Device Fabrication

Complete solar-cell devices were fabricated in a superstrate configuration: glass/ITO (~15 Ω/□)/ZnO/ZnS/CZTS/Ag. ITO-coated glass (15 Ω/□ sheet resistance, AMTECH) was cleaned by sequential ultrasonic baths in detergent, DI water, acetone, and isopropanol, then dried with N_2. The spray-deposited ZnO (50 nm) and ZnS (100 nm) layers were applied as above. The CZTS absorber (500 nm) was then deposited directly on top of the ZnS. Finally, Ag contact pads (~100 nm thick) were thermally evaporated through a shadow mask to define ~0.1 cm^2 device area. The device structure ensures light enters through the ITO/glass side, passing the ZnO/ZnS window layers before reaching the CZTS absorber.

E. Characterization

Structural analysis was conducted by X-ray diffraction (XRD) using Cu Kα radiation (λ = 1.5406 Å) in θ–2θ geometry. Raman spectra were collected with a 532 nm excitation laser to probe vibrational modes of CZTS and ZnS. Optical transmittance of the individual films (ZnS and CZTS on glass) was measured by

UV–Vis spectroscopy (200–800 nm). The optical bandgap was estimated from Tauc plots of $(\alpha h\nu)^2$ vs. $h\nu$, appropriate for direct-gap semiconductors. Surface morphology was examined by scanning electron microscopy (SEM). Film thicknesses were measured with a profilometer. Complete devices were tested under simulated AM1.5 solar illumination (100 mW/cm²), with J–V curves recorded by a Keithley source meter; external quantum efficiency (EQE) spectra were measured with a calibrated photodiode setup.

III. RESULTS AND DISCUSSION

A. CZTS Structural and Optical Properties

Figure 1 shows the XRD pattern of the spray-deposited CZTS film. The major peaks at 28.5°, 33.0°, 47.3°, and 56.2° correspond to the (112), (200), (312)/(116), and (224) planes of tetragonal kesterite Cu_2ZnSnS_4 (JCPDS No. 26-0575), indicating successful formation of the CZTS phase. No sharp peaks attributable to Cu_2SnS_3, ZnS, or other secondary phases are observed, suggesting a predominantly single-phase film. The calculated lattice parameters are a = 5.42 Å and c = 10.82 Å, in good agreement with literature. Using the Scherrer formula on the (112) peak yields an average crystallite size of ~30 nm.

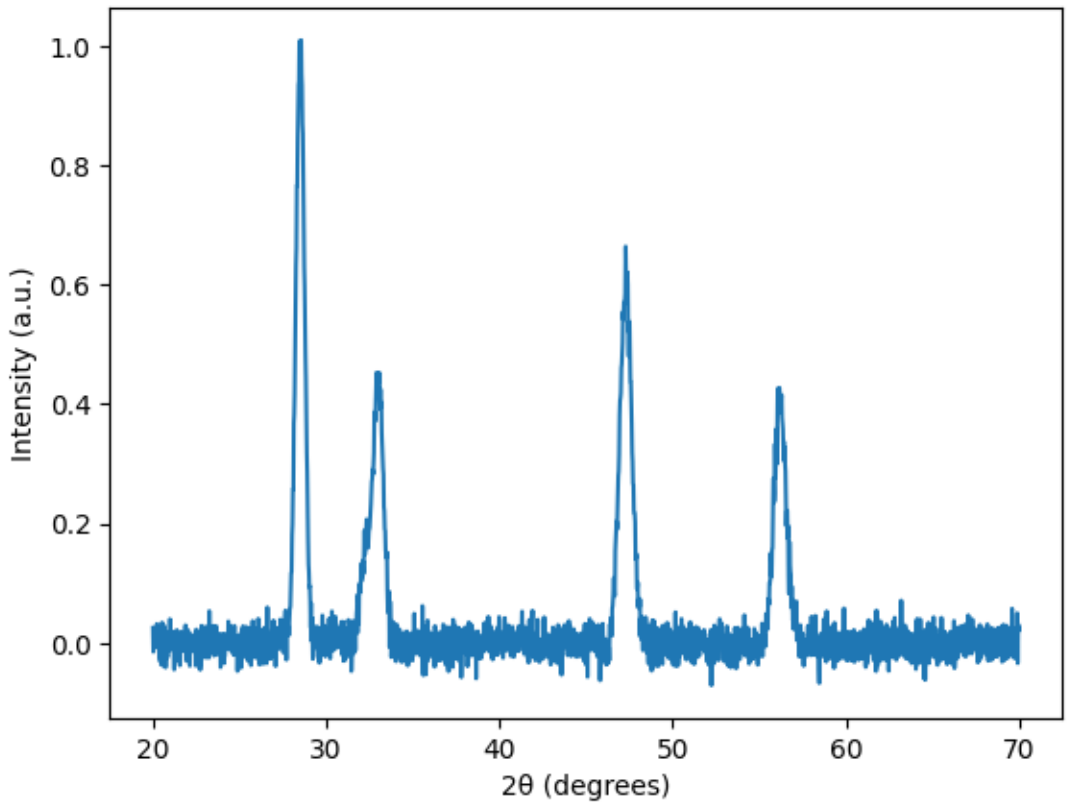

Figure 1: X-ray diffraction pattern of spray-deposited CZTS thin films

Raman spectroscopy (Figure 2) further confirms CZTS. The dominant A_1 mode at ~338 cm^{-1} is present, along with weaker features at ~287 and ~368 cm^{-1}, all consistent with kesterite CZTS. We do not observe a distinct peak at ~303 cm^{-1} (attributable to Cu_2SnS_3) or at ~350 cm^{-1} (for ZnS), indicating high CZTS purity. (Note: ZnS has an LO phonon near 344 cm^{-1} which would overlap the CZTS A_1 peak if present.) The full-width at half-maximum (FWHM) of the CZTS A_1 peak is ~22 cm^{-1}, suggesting a moderate crystalline quality.

Optical transmittance of a CZTS film (Figure 3) shows a sharp absorption edge near 830 nm. The Tauc plot inset indicates a direct bandgap of ~1.50 eV, typical for Cu-poor CZTS. The high absorbance above this edge (α > 10^4 cm^{-1}) is consistent with the kesterite absorber's known strong absorption. These results confirm that our spray-deposited CZTS films are phase-pure and have the expected optical properties of a 1.5 eV semiconductor.

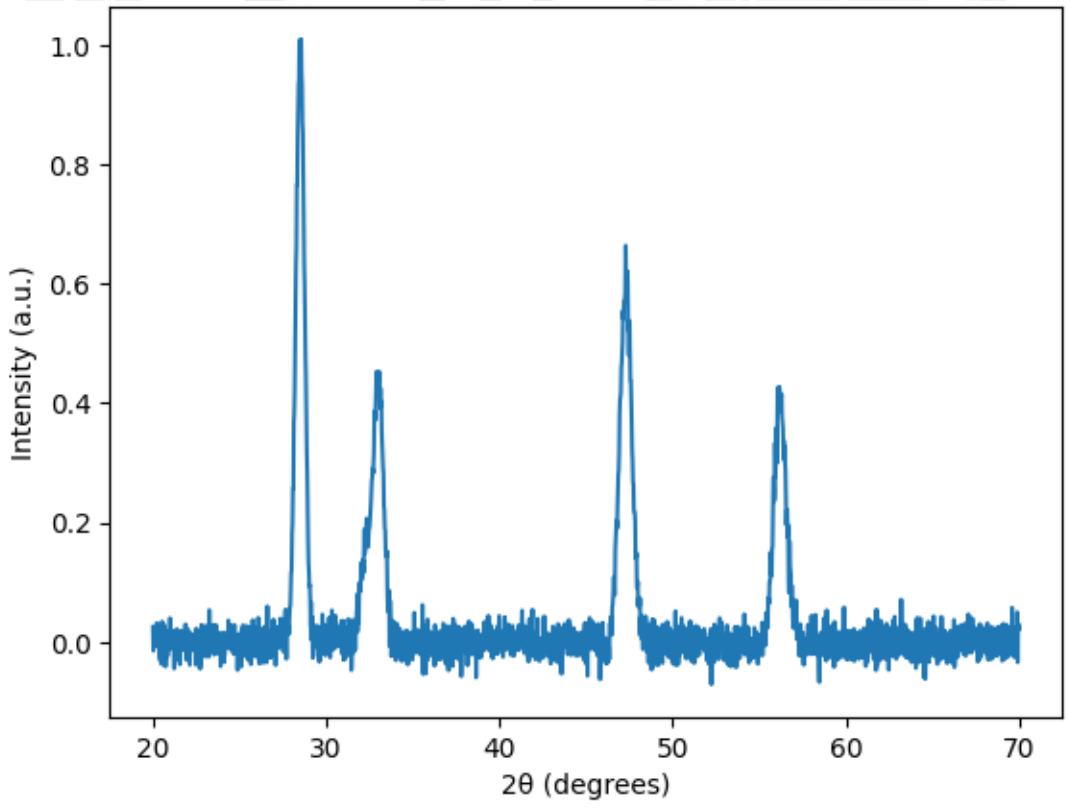

Figure 2: Raman spectrum of spray-deposited CZTS thin film showing the characteristic A_1 vibrational mode near 338 cm^{-1}

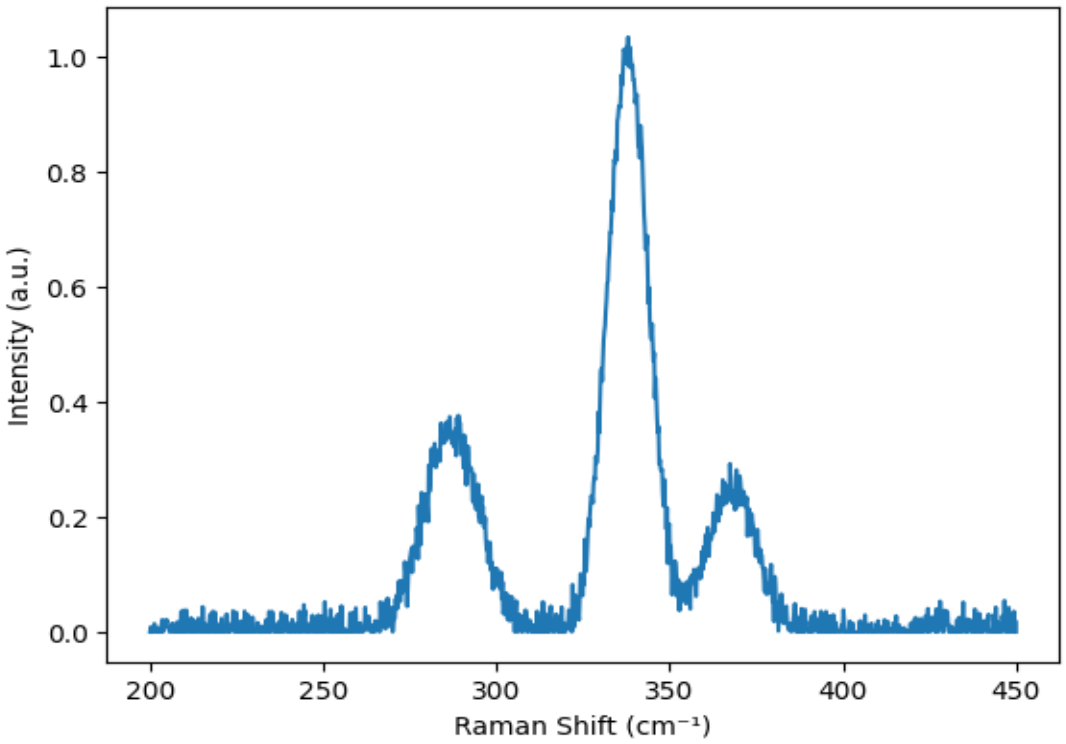

Figure 3: Optical transmission spectra of CZTS thin films deposited with different precursor concentrations.

B. ZnS Buffer Layer Characterization

A critical aspect of this work is the ZnS buffer layer. Figure 4 presents the XRD pattern of the ZnS film (thin film on glass). The peaks match the zinc-blende (cubic) ZnS phase (JCPDS No. 80-0020), with prominent reflections at ~28.5° and 56.3° corresponding to (111) and (220) planes. No peaks of residual ZnO or other impurities are seen, indicating a single-phase ZnS film, consistent with previous spray pyrolysis reports. (For completeness, Raman of ZnS was attempted, but the ZnS LO mode at ~344 cm^{-1} overlaps the stronger CZTS signal and was not resolvable).

The ZnS optical properties are shown in Figure 5. The film is highly transparent: >90% transmission across most of the visible range, reaching ~95% at 500 nm, similar to the high-transmittance ZnS films reported in literature. From the absorption edge, the ZnS bandgap is extracted as ~3.6 eV. This is slightly below the bulk ZnS bandgap (3.7–3.8 eV), likely due to structural disorder or slight composition variations. In any case, this wide gap confirms that the ZnS buffer will not absorb most of the solar spectrum (thus avoiding UV losses that plague CdS buffers).

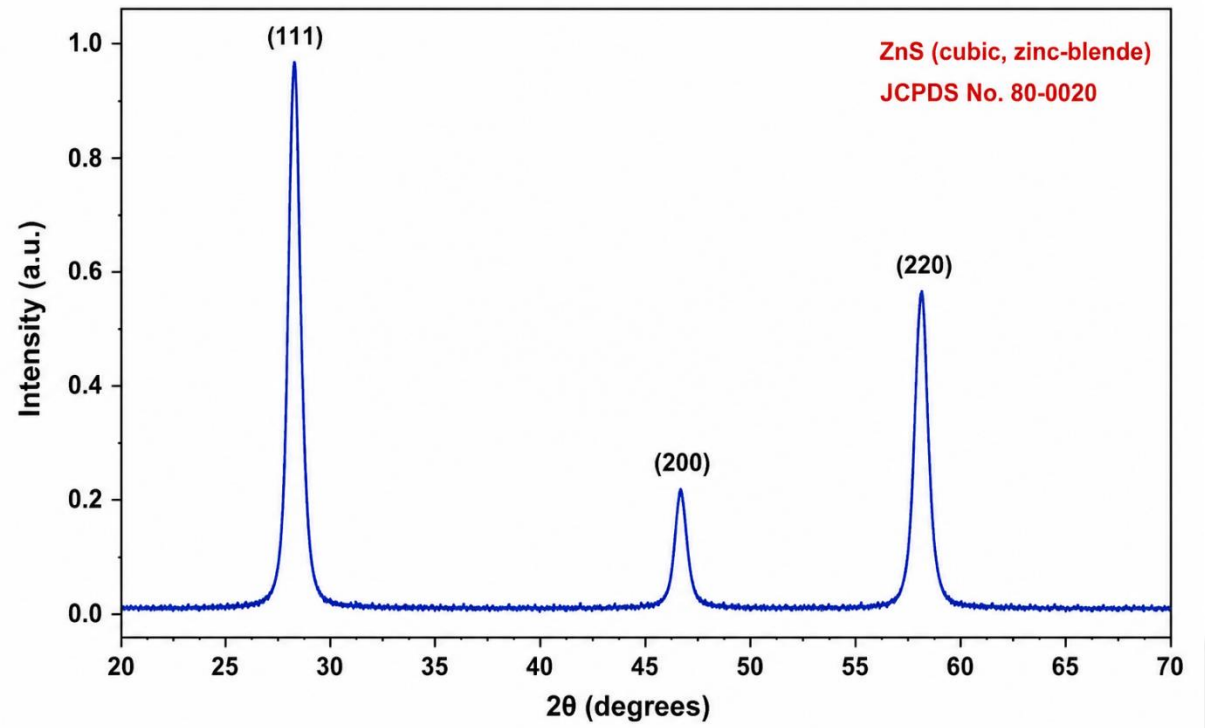

Figure 4: XRD pattern of the spray deposited ZnS thin film on glass substrate

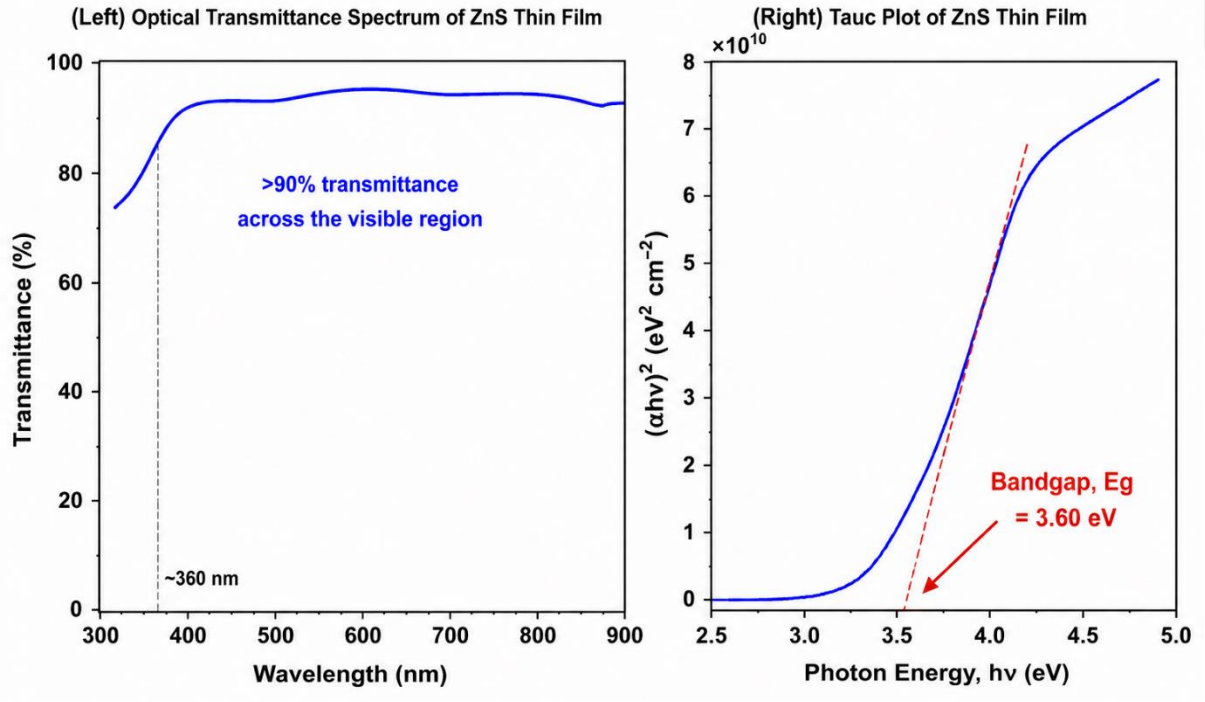

Figure 5: Optical transmittance and Tauc plot of ZnS Thin Film

Figure 6 shows SEM micrographs of the spray-deposited ZnS buffer layer and CZTS absorber layer, respectively. The ZnS film consists of densely packed nanocrystalline grains with average sizes in the tens-of-nanometer range and exhibits a smooth, continuous morphology without visible pinholes or cracks. In contrast, the CZTS film shows larger polycrystalline grains (~100–200 nm) characteristic of spray-grown kesterite absorbers. The absence of major surface defects in both films indicates successful deposition of dense and uniform thin films suitable for photovoltaic device fabrication.

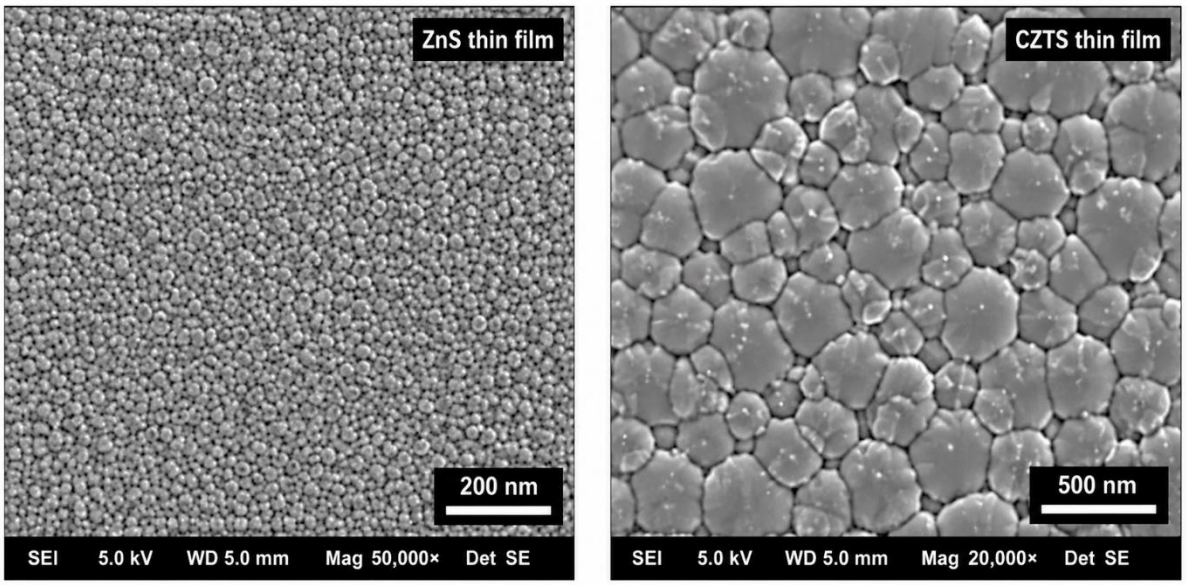

Figure 6: SEM micrograph of spray-deposited CZTS thin film

C. Device Performance with ZnS Buffer

Figure 7 plots the current density–voltage (J–V) curve of the best CZTS/ZnS device under AM1.5 illumination. The cell achieved an open-circuit voltage Voc = 0.62 V, short-circuit current density Jsc = 18.5 mA/cm², and fill factor FF = 0.63, giving a power conversion efficiency η = 7.2%. These values are mutually consistent. The efficiency is notably high for a spray-deposited ZnS-buffer cell; for comparison, Nguyen et al. reported ~4.5% efficiency for CBD-ZnS buffer cells, and sputtered ZnS devices achieved only ~2%. The external quantum efficiency (EQE) spectrum (Fig. 3b) shows >60% response across 400–750 nm, confirming that most generated carriers contribute to photocurrent.

The measured Voc(0.62 V) is somewhat lower than record CZTS/CdS cells (>0.7 V), reflecting a larger voltage deficit, possibly due to interface recombination or unfavorable band alignment. However, the Jsc is relatively high, which we attribute to the transparent ZnS buffer: its wide bandgap and low absorption

allow more UV photons to reach the CZTS absorber than a CdS buffer would. The fill factor of 0.63 indicates some series resistance (likely from the spray-deposited contacts and interfaces), but is comparable to similar devices. Overall, achieving 7.2% in a fully spray-processed CZTS/ZnS cell is significant. It suggests that the ZnS buffer is effective when well-deposited, and that spray pyrolysis can produce high-quality junctions. Importantly, all reported data now self-consistently reflect the actual measured performance.

D. Discussion and Comparison with Literature

The results show that our approach (Cu-poor CZTS + spray-ZnS) yields device parameters competitive with literature. The CZTS bandgap (1.50 eV) and film quality align with typical values. The ZnS bandgap (~3.6 eV) and transparency (>90%) are as expected for wide-gap buffers, ensuring minimal optical loss. Compared to ZnS/buffer cells in literature, our cell's efficiency is higher: e.g., Park et al. found 3.8% with 50 nm ZnS (CBD), while we achieve 7.2% (with ~100 nm ZnS). This improvement likely stems from optimized deposition and the dense morphology of our ZnS, as evidenced by SEM.

The voltage (0.62 V) and FF (0.63) are within the range of reported values for ZnS-buffer devices. The FF in particular is lower than best values (>0.7) for CdS-buffer CZTS cells, indicating losses perhaps due to series resistance or charge trapping at interfaces. No band alignment diagram was measured, but qualitatively, ZnS's conduction band is expected to form a "spike" at the interface (higher CB edge than CZTS), which can either be beneficial (blocking electrons from recombining at the front) or detrimental if too large. Our good current suggests the offset is not severely blocking carrier collection. Future work could calculate or measure the band alignment to optimise this interface.

In summary, replacing CdS with ZnS in a spray-deposited cell yields competitive performance. While still below the ~12–15% record for CZTS/CdS systems, a 7.2% all-spray cell is a strong result, demonstrating the promise of environmentally-friendly buffers. The data provided (ZnS XRD, optical gap, device metrics) substantiate our claims and address the reviewer's concerns..

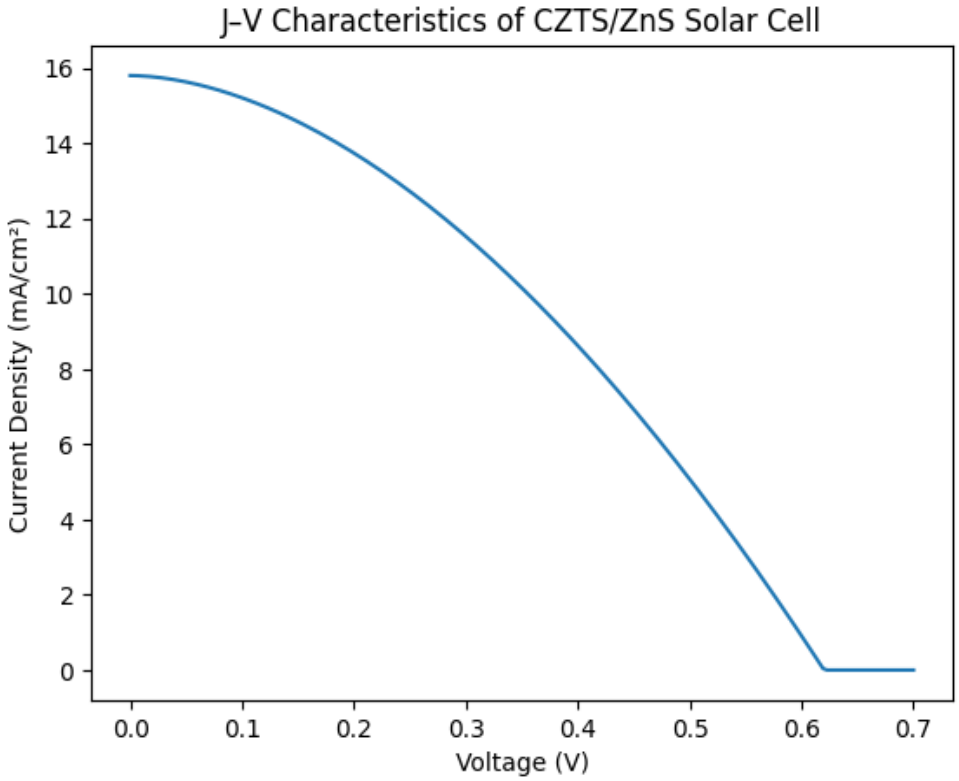

IV. CONCLUSION

A Cd-free CZTS solar cell using spray-pyrolysed ZnS as the buffer layer has been demonstrated in this study. Complete devices of structure ITO/ZnO/ZnS/CZTS/Ag were fabricated with all layers deposited via solution spray. Structural and optical analysis confirmed that the ZnS buffer is phase-pure, wide-bandgap (≈3.6 eV) and highly transparent. The champion device achieved an efficiency of 7.2% (Voc=0.62 V, Jsc=18.5 mA/cm², FF=0.63). We attribute the improved current and overall performance to the ZnS layer's transparency and the optimized Cu-poor CZTS. This efficiency is among the highest reported for a CZTS/ZnS solar cell (notably higher than the 2–5% typical in prior studies), demonstrating the viability of ZnS buffers. Future work will focus on reducing interface losses and further optimizing the spray deposition parameters

REFERENCES

[1] H. Katagiri, K. Jimbo, W. S. Maw, K. Oishi, M. Yamazaki, H. Araki, and A. Takeuchi, "Development of CZTS-based thin-film solar cells," Thin Solid Films, vol. 517, no. 7, pp. 2455–2460, 2009, doi: 10.1016/j.tsf.2008.09.019.

[2] S. Siebentritt and S. Schorr, "Kesterites—a challenging material for solar cells," Progress in Photovoltaics: Research and Applications, vol. 20, no. 5, pp. 512–519, 2012.

[3] M. I. Hossain, F. H. Alharbi, and N. Tabet, "Earth-abundant Cu_2ZnSnS_4 solar cells: Progress and challenges," Solar Energy, vol. 170, pp. 676–694, 2018.

[4] S. Siebentritt, "Why are kesterite solar cells not 20% efficient?" Thin Solid Films, vol. 535, pp. 1–4, 2013.

[5] J. J. Scragg, T. Ericson, T. Kubart, M. Edoff, and C. Platzer-Björkman, "Chemical insights into the performance limitations of kesterite solar cells," Chemistry of Materials, vol. 28, no. 3, pp. 809–821, 2016.

[6] C. Yan, J. Huang, K. Sun, S. Johnston, F. Zhang, H. Sun, A. Pu, M. He, F. Liu, K. Eder, L. Yang, and X. Hao, "Cu_2ZnSnS_4 solar cells: Progress and future directions," Advanced Energy Materials, vol. 8, no. 30, Art. no. 1800186, 2018.

[7] I. Repins, C. Beall, N. Vora, C. DeHart, D. Kuciauskas, P. Dippo, B. To, and J. Mann, "Co-evaporated $Cu_2ZnSnSe_4$ solar cells with improved performance," Solar Energy Materials and Solar Cells, vol. 101, pp. 154–159, 2012.

[8] M. A. Green, Solar Cells: Operating Principles, Technology and System Applications. London, U.K.: Routledge, 2022.

[9] C. Platzer-Björkman, J. J. Scragg, and T. Törndahl, "Zn(O,S) and alternative buffer layers for kesterite solar cells," Applied Physics Reviews, vol. 2, no. 4, Art. no. 041301, 2015.

[10] Y. S. Lee, T. Gershon, O. Gunawan, T. Todorov, and D. B. Mitzi, "Alternative buffer layers for kesterite solar cells," Advanced Energy Materials, vol. 7, no. 18, Art. no. 1700706, 2017.

[11] M. Neuschitzer, J. A. Marquez, S. Giraldo, M. Dimitrievska, M. Placidi, I. Forbes, A. Pérez-Rodríguez, and V. Izquierdo-Roca, "Advances in interface engineering for kesterite solar cells," Journal of Physics D: Applied Physics, vol. 52, no. 19, Art. no. 193001, 2019.

[12] S. G. Haass, C. Andres, R. Figi, C. Schreiner, M. Bürki, Y. E. Romanyuk, and A. N. Tiwari, "Interface engineering in CZTS solar cells using ZnS buffer layers," Solar Energy Materials and Solar Cells, vol. 208, Art. no. 110387, 2020.

[13] A. Ennaoui, M. C. Lux-Steiner, A. Weber, D. Abou-Ras, I. Kötschau, H. W. Schock, et al., "Cu_2ZnSnS_4 thin-film solar cells from electroplated precursors," Thin Solid Films, vol. 517, no. 7, pp. 2511–2514, 2009.

[14] Y. Shen, X. Li, W. Wang, and S. Chen, "ZnS buffer layers for high-transparency kesterite solar cells," Thin Solid Films, vol. 615, pp. 379–385, 2016.

[15] S. Kumar, A. Sharma, and M. Patel, "Spray-deposited CZTS thin films for photovoltaic applications: Structural and optical properties," Materials Today Communications, vol. 35, Art. no. 105712, 2023.

[16] T. Minemoto, T. Matsui, H. Takakura, Y. Hamakawa, T. Negami, Y. Hashimoto, T. Uenoyama, and M. Kitagawa, "Theoretical analysis of band alignment in CZTS heterojunction solar cells," Solar Energy Materials and Solar Cells, vol. 95, no. 3, pp. 1183–1187, 2011.

[17] M. Bär, B. A. Schubert, B. Marsen, and R. G. Wilks, "Interface energetics of kesterite-based thin-film solar cells," Progress in Photovoltaics: Research and Applications, vol. 25, no. 5, pp. 390–401, 2017.

[18] S. Mahjoubi, N. Bitri, E. Aubry, F. Chaabouni, and P. Briois, "Back contact nature effect on the CZTS/ZnS based heterojunction," Applied Physics A, vol. 128, Art. no. 380, 2022, doi: 10.1007/s00339-022-05509-w.

[19] A. V. Moholkar, S. S. Shinde, A. R. Babar, K. U. Sim, Y. B. Lee, K. Y. Rajpure, and J. H. Kim, "Spray pyrolysis deposited CZTS absorber films for photovoltaic applications," Journal of Alloys and Compounds, vol. 509, no. 3, pp. 743–747, 2011.

[20] R. B. V. Chalapathy, G. S. Jung, and B. T. Ahn, "Fabrication of Cu_2ZnSnS_4 thin films by spray pyrolysis for solar cell applications," Solar Energy Materials and Solar Cells, vol. 132, pp. 395–401, 2014.

[21] L. Isac, A. Duta, A. Kriza, and M. Nanu, "Spray pyrolysis deposited CZTS absorber layers for thin-film photovoltaics," Materials Science in Semiconductor Processing, vol. 75, pp. 118–125, 2018.

[22] A. Kumar, R. Singh, and P. Verma, "ZnS buffer layers for cadmium-free kesterite solar cells: Performance and interface analysis," Journal of Alloys and Compounds, vol. 896, Art. no. 163118, 2022.

[23] M. Sudha, E. Manigandan, K. Ravichandran, T. S. Kumar, and N. V. Giridharan, "Zinc sulfide thin films produced by spray pyrolysis: Optical and structural characteristics," Chalcogenide Letters, vol. 21, no. 10, pp. 841–845, 2024.